



THE PSEUDOELASTICITY AND THE SHAPE MEMORY EFFECT IN CoNiAl ALLOYS

Jaromír Kopeček^{1,*}, Markéta Jarošová², Karel Jurek², Oleg Heczko¹

¹ Institute of Physics AS CR, Na Slovance 2, Praha 8, 182 21, Czech Republic.

² Institute of Physics AS CR, Cukrovarnická 10/112, 162 00, Praha 6, Czech Republic

* corresponding author: e-mail: kopecek@fzu.cz:

Resume

The cobalt alloys (close to the CoNiAl stoichiometry) are the less known shape memory alloys. Such behavior is consequence of the martensitic transformation. The pseudoelasticity is caused by the stress-induced martensitic transformation above the equilibrium martensite start temperature from high temperature cubic phase (austenite) to lower symmetry phase (martensite). In CoNiAl the pseudoelastic behavior can be obtained by the high temperature annealing. In presented work the effect of the annealing temperature on both pseudoelastic behavior and microstructure was investigated.

Article info

Article history:

Received 30 January 2013

Accepted 17 November 2013

Online 28 February 2014

Keywords:

Shape memory alloys;

Co-alloys;

Metallography;

Martensitic transition;

Stress induced martensite.

Available online: <http://fstroj.uniza.sk/journal-mi/PDF/2014/06-2014.pdf>

ISSN 1335-0803 (print version)

ISSN 1338-6174 (online version)

1. Introduction

1.1. History of shape memory effect

The shape memory effect was observed for the first time in 1936 by Ölander [1], but the physical nature was unknown till 1951 [2]. Those years connection between observed “pseudoplasticity” and martensitic transformation was understood in couple of alloys, including Ölander’s AuCd. This remained academic curiosity until the same effect was observed in nearly stoichiometric NiTi alloy in 1963 [3] and its application in 1971 – the couplings on fuel piping in wings of F-14 fighter. Later shape memory alloy were applied in wide range of products. Very important for the research was breakthrough in medical applications connected with proven biocompatibility of Nitinol (commercial name of NiTi alloy).

The explanation of the shape memory effect is very simple from present-day point of view. During cooling the original, high-

temperature, high-symmetric phase (called austenite) transforms into the low-temperature, lower-symmetric phase (called martensite). The consequence of such transition is the formation of orientation domains (variants) connected by twin boundaries. They are distributed equally if system is not under any external force. The mechanical stress leads to redistribution of variants’ populations, because the low-symmetric cell has different length in different crystallographic directions. On macroscopic level we then observe large shape change. Following heating over the reverse martensitic temperature induces back the high-temperature phase and all variants change into the original elementary cell. Thus original shape appears again. The necessary conditions for the effect are the martensitic transformation resulting in variants formation and mobile twin variants’ boundaries that allow variant redistribution due to applied stress.

Going back to original observations, one should mention that it was not shape memory

effect, which surprised Ölander in sample preparation for his electrochemical study. What he actually saw was “rubber like behavior” – extreme prolongation of metallic rod and he named it “pseudoplasticity”. Nowadays the effect is called pseudoelasticity as it is caused by the (reversible) stress induced martensitic transformation. Such transformation can be induced by mechanical stress (or other external force) in the vicinity of thermodynamically equilibrium transformation temperature. The required energy for stress-induced transformation is provided by external stress and the system lowers its energy as it deforms in external stress direction.

The shape memory effect caused by martensitic transformation is not rare occasion, but the most widely studied and applicable alloys are just few: NiTi and CuAlNi. Recently, new attention is focused to the development of the nickel-free alloys for medical application; mainly we spoke about Ti-Ta and Nb-Ti systems.

1.2. Magnetically induced shape memory effect

The real revolution in slightly stagnating field of shape memory alloys was caused by the discovery of magnetically induced shape memory effect (MSM) [4]. It was found in ferromagnetic Ni₂MnGa alloy and observed shape change has been growing from 0.2 % in 1996 [4] up to 10 % in 2002 [5, 6]. The magnetic field is usually thought to be weak in comparison with effect of temperature or stress, but under special conditions the structural redistribution of martensitic variants and the martensitic transformation itself can be caused by the magnetic field [7]. The essential for the magnetically induced reorientation is the high magnetic anisotropy and low twinning stress, which allow variants' reorientation [5, 8]. The combination of required properties is unique that is why the original Ni-Mn-Ga, Ni-Mn-In and Fe-Pd are only alloys exhibiting significant effect of magnetic field on martensitic transformation or variants redistribution. It

seems that the necessary condition for MSM is modulation of martensite [9].

1.3. Co-Ni-Al system

The ferromagnetic alloys from Co-Ni-Al system were chosen as attractive candidates for magnetic shape memory applications as these alloys exhibit both the martensitic transformation and ferromagnetic-paramagnetic transition [10]. They were supposed to have the higher transformation stresses and the wider interval of superelasticity than other shape memory alloys (SMA). The Co-Ni-Al and mainly Co-Al systems have been investigated since the second half of 20th century as their creep properties are excellent [11]. Nevertheless, the brittleness was not overcome in these alloys which limited their application. The original expectation of magnetic shape memory effect was also not satisfied completely, although the MSM was observed but the shape change was just 0.06 % [12], which on the other hand can be just ordinary magnetostriction.

The phase diagram of Co-Ni-Al system was established and seems not to be complicated [13]. The area with high content of cobalt contains just three of phases. The A1, disordered fcc cobalt solid solution (space group Fm3m) and B2, ordered phase (space group Pm3m) and L1₂, ordered phase, which appears in high nickel alloys. This L1₂ phase is ordered superstructure of A1 phase [14]. There was observed martensitic transformation of B2 phase into the tetragonal L1₀ phase [15]. The described transformation kinetics is similar to Ni-Al system [15].

We investigated alloy with particular composition Co₃₈Ni₃₃Al₂₉. The high-temperature state of such alloy (i.e. prior the martensitic transformation) is two phase mixture of A1 and B2 phases. Such microstructure is unusual in SMAs. The A1 phase, which forms interdendritic particles, is supposed to compensate transformation and thermal stresses [10]. Its content does not

change during martensitic transformation and at temperatures below it [10, 16]. The microstructure development during the cooling from melt is quite complicated in contrast with the simple phase composition and it is very sensitive to the composition and thermomechanical history of the sample [17].

To study the shape memory effect one needs the single-crystalline samples to establish orientation dependence of transformation stresses. The single-crystalline samples were annealed for homogenization in all published works. There is a surprisingly wide scattering in both times and temperatures of homogenization annealing. The older works used the annealing at temperatures 1100 °C up to 1350 °C up to 24h [12, 18], later the annealing times was shortened to 4 h [19]. We searched for the shortest period of homogenization annealing and tested the 1 h of annealing at 1250 °C and 1350 °C.

2. Sample preparation

The $\text{Co}_{38}\text{Ni}_{33}\text{Al}_{29}$ polycrystalline alloy was used to prepare single-crystals. The Bridgman and floating-zone methods were used [20]. The low pulling rates (below $10 \text{ mm}\cdot\text{h}^{-1}$) lead to the disintegration of the crystal body into two-phase mantle and single-phase core, which is undesirable structure [20]. The higher pulling rates in Bridgman method gave the same composition of the matrix and particles, although the structure along the crystal was not homogeneous [21]. Finally, the pulling rate $104 \text{ mm}\cdot\text{h}^{-1}$ produced homogeneous distribution of the A1 particles within the B2 matrix. Such microstructure is the only one suitable for the repeatable samples' preparation.

The samples for annealing study were cut from the bottom of Bridgman crystal (i.e. the last solidified part of material). The outer cylindrical segment was metallographically prepared as a reference sample. The cuboidal samples were cut from the adjacent belt of cylindrical sample. The samples were annealed and quenched into the cold water.

Then samples were cut along the side diagonal using spark cutting machine, mounted into the resin and metallographically polished. The sketch of the samples' cut can be seen in Fig. 1.

3. Description of achieved results

The observed microstructures of as-cast sample consisted of two phases. The big unidirectional grains of B2 matrix were covered with the interdendritic particles of A1 phase, Fig. 2. Some voids and shrinkage cavities were also presented as the samples were cut from the bottom of the grown crystal.

The microstructure of the sample annealed at 1250 °C and quenched remained the same, but the microstructure of the sample annealed at 1350 °C was changed and all A1 particles were dissolved, Fig. 3. The composition of both samples was spatially stable. There was not visible any tendency to segregation of any element at the outer part of the crystal. The composition is the same in both crystals on outer surface of quenched sample and in the middle of it. This proves important notion that the one hours annealing is sufficient for both temperatures. The composition measured in the matrix of sample annealed at 1250 °C agreed with the composition of other crystals grown $104 \text{ mm}\cdot\text{h}^{-1}$ pulling rate [19]. One disturbed point on the line B taken at the sample annealed at 1250 °C is caused by the A1 particle, as the composition fits with other measurement of A1 particles [21]. The measured data confirmed that above certain pulling rate the composition of matrix and particles remained the same and just the ratio of phases drive the composition of whole material, Fig. 4a. The sample annealed at 1350 °C had one phase microstructure, A1 particles were dissolved, however the aluminum content seems to be 4 at.% higher than in as grown material. As the content of both transition metals decrease was the same, we expect the systematic shift in calibration of the energy-dispersion spectra, Fig. 4b.

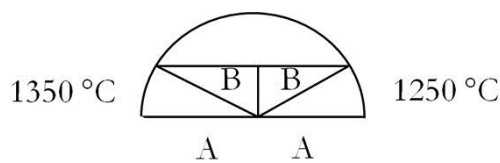


Fig. 1. The sketch of the samples' cut.

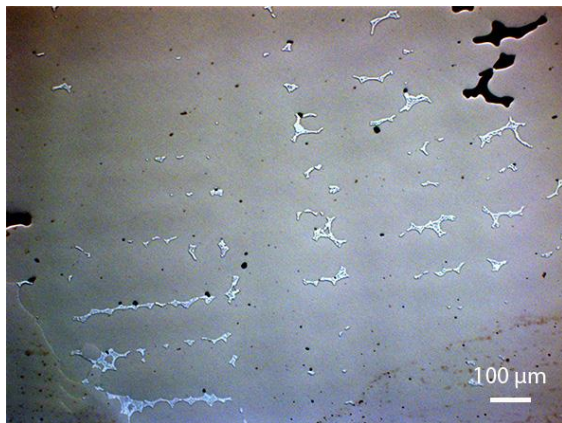
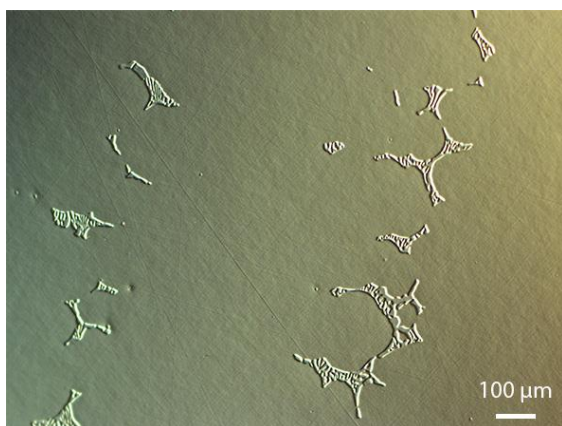
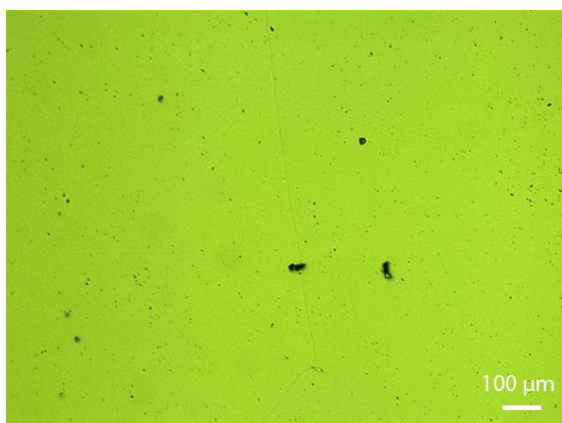


Fig. 2. Structure of as-grown sample prepared by Bridgman method with the pulling rate $104 \text{ mm}\cdot\text{h}^{-1}$ (full colour version available online)



a) $1250 \text{ }^\circ\text{C}$



b) $1350 \text{ }^\circ\text{C}$

Fig. 3. The microstructure of annealed and quenched samples at a) $1250 \text{ }^\circ\text{C}$ and b) $1350 \text{ }^\circ\text{C}$. (full colour version available online)

4. Discussion

The literature survey gave surprisingly long times for homogenization annealing from whole days [12, 18] down to couple of hours [10, 19]. The various annealing times depends probably on the initial microstructure, because the solidification routes in Co-Ni-Al system are complicated [17], each author develop own strategy depending on the initial microstructure. Samples used in this study were homogeneous [20, 21] and 1 h of annealing was found to be sufficient.

There should be mentioned important observation: high-temperature annealing and quenching is not just matter of homogenization. The significant redistribution of elements happened at this process and it is not just the dissolving of Al particles. The more subtle changes must take place in matrix as both applied annealing procedures lead to pseudoelastic behavior, whereas the initial as grown samples exhibit no such behavior [22]. The changes can be connected with the dissolving of Al particles and enhancement of the matrix with cobalt and nickel atoms. When such matrix, rich on Co and Ni, is quenched, the matrix begin to decompose and some nanoprecipitates can be formed. The Al face centered cubic nanoprecipitates were observed in material prepared with the pulling rate $28 \text{ mm}\cdot\text{h}^{-1}$, which was not pseudoelastic [23] and hexagonal close packed nanoprecipitates were observed in material prepared with the pulling rate $38 \text{ mm}\cdot\text{h}^{-1}$, which was pseudoelastic [24]. Also other types of nanoprecipitates are described in literature [25]. The process is believed to be fundamental for understanding of pseudoelastic behavior, but the exact description is still missing.

Nevertheless, the nanoprecipitation of the excess cobalt and nickel atoms in the B2 matrix can be the process, which complicate or even suppress the formation of dislocation and the deformation mechanism must proceed differently i.e. by twinning, thus support spreading of stress-induced martensite needles.

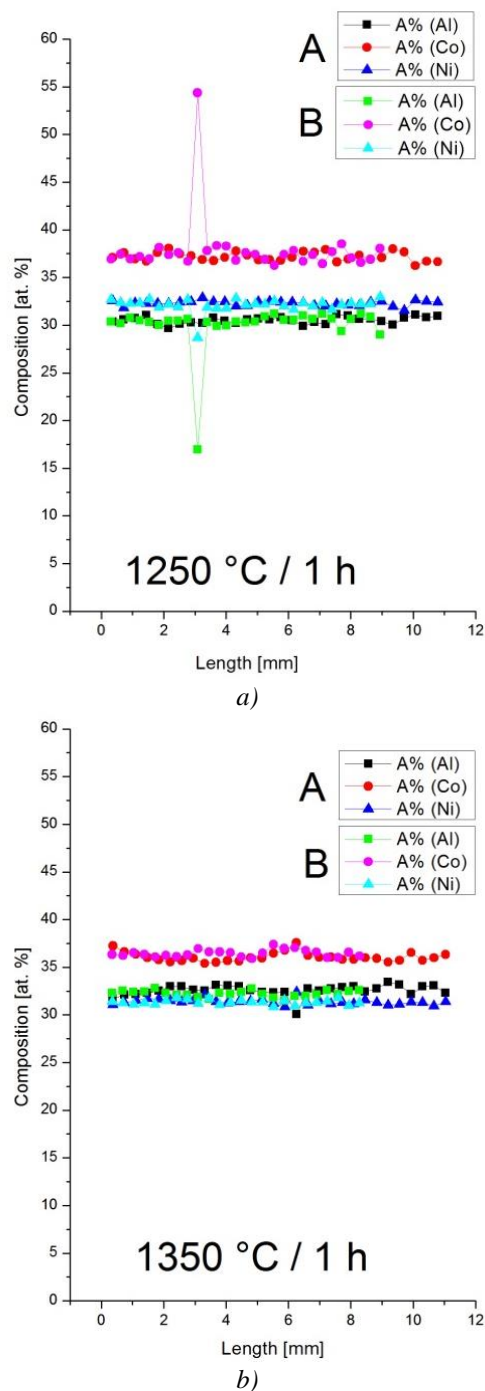


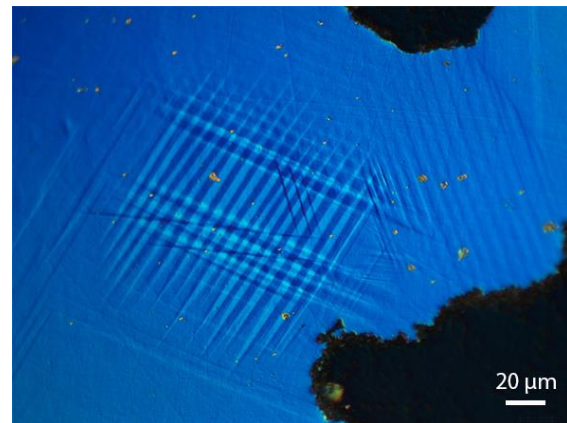
Fig. 4. The composition of quenched samples obtained by EDS along the side (A) and the diagonal (B) of the cuboidal samples. The annealing temperatures are noticed in respective graphs. (full colour version available online)

Although the equilibrium martensitic transformation in studied alloy was found to be close to $-70\text{ }^{\circ}\text{C}$ by in-situ neutron diffraction [16] and magnetic susceptibility measurements [22], the stress-induced martensitic lamellae in both annealed samples were observed at room

temperature. These martensite needles, however, just appeared in the special positions with the constrained geometry – usually close to thin edges or in free dendritic arms, Fig. 5. It points that free surface or particles are sources of stresses, which helps stress-induced martensite to develop.



a)



b)

Fig. 5. The stress induced martensitic lamellae on confined geometries at room temperature. (full colour version available online)

5. Conclusions

The $\text{Co}_{38}\text{Ni}_{33}\text{Al}_{29}$ ferromagnetic shape memory alloy single-crystals were prepared using Bridgman method. Such unidirectional solidified samples were annealed one hour at $1250\text{ }^{\circ}\text{C}$, respectively $1350\text{ }^{\circ}\text{C}$ and quenched. Both used procedures are sufficient to the formation of the structure which exhibits pseudoelastic behavior. The stress induced martensite lamellae were observed in both samples in the special, confined geometries.

Acknowledgment

Authors would like to acknowledge the financial support from the Czech Science Foundation project 101/09/0702..

References

- [1] J. Ölander., J. Am. Chem. Soc. 54(10) (1939) 3819-3833.
- [2] L.C. Chang, T.A. Read: Trans. AIME, 191(1) (1951) 47-52.
- [3] W.J. Buehler, J.V. Gilfrich, R.C. Wiley: J. Appl. Phys. 34(5) (1963) 1475-1477.
- [4] K. Ullakko, J.K. Huang, C. Kantner, R.C. O'handley, V.V. Kokorin: Appl. Phys. Lett., 69(13) (1996) 1966-1968.
- [5] O. Heczko, A. Sozinov, K. Ullakko: IEEE Trans. Mag. 36(5) (2000) 3266-3268.
- [6] A. Sozinov, A.A. Likhachev, N. Lanska, K. Ullakko: Appl. Phys. Lett. 80(10) (2002) 1746-1748.
- [7] R. Kainuma, Y. Imano, W. Ito, Y. Sutou, H. Morito, S. Okamoto, O. Kitakami, K. Oikawa, A. Fujita, T. Kanomata, K. Ishida: Nature 439(7079) (2006) 957-970
- [8] O. Heczko, N. Scheerbaum, O. Gutfleisch: In: Nanoscale Magnetic Materials and Applications, Eds: J.P. Liu, E. Fullerton, O. Gutfleisch, D.J. Sellmyer, Springer Science+Business Media, LLC New York 2009, pp. 14-1.
- [9] S. Kaufmann, U. K. Roßler, O. Heczko, M. Wuttig, J. Buschbeck, L. Schultz, S. Fahler: Phys. Rev. Lett. 104(14) (2010) 145702-1-4
- [10] K. Oikawa, L. Wulff, T. Iijima, F. Gejima, T. Ohmori, A. Fujita, K. Fukamichi, R. Kainuma, K. Ishida: Appl. Phys. Lett., 79(20) (2001) 3290-3292.
- [11] L.A. Hocking: J. Inst. Met. 99(1) (1971) 98-101.
- [12] H. Morito, A. Fujita, K. Fukamichi, R. Kainuma, K. Ishida, K. Oikawa: Appl. Phys. Lett. 8(9) (2002) 1657-1659.
- [13] M. Hubert-Protopescu, H. Hubert: In: Ternary alloys: a comprehensive compendium of evaluated constitutional data and phase diagram. Vol. 4: Al-Cd-Ce to Al-Cu-Ru, Eds: G. Petzow, G. Effenberg, VCH Weinheim 1991, pp. 234-244.
- [14] Information about particular structures on: <http://cstwww.nrl.navy.mil/lattice/index.html>.
- [15] Y. Murakami, D. Shindo, K. Oikawa, R. Kainuma, K. Ishida: Acta Mater. 50(8) (2002) 2173-2184.
- [16] J. Kopeček, F. Yokaichiya, F. Laufek, M. Jarošová, K. Jurek, J. Drahokoupil, S. Sedláková-Ignáčová, P. Molnár, O. Heczko: Acta Phys. Pol. A 122(3) (2012) 475-477.
- [17] R. Kainuma, M. Ise, C.C. Jia, H. Ohtani, K. Ishida: Intermetallics 4(S1) (1996) S151-S158.
- [18] H.E. Karaca, I. Karaman, D.C. Lagoudas, H.J. Maier, Yu.I. Chumlyakov: Scripta Mater. 49(9) (2003) 831-836.
- [19] J. Liu, H. Zheng, Y. Huang, M. Xia, J. Li: Scripta Mater. 53(1) (2005) 29-33.
- [20] J. Kopeček, K. Jurek, M. Jarošová, J. Drahokoupil, S. Sedláková-Ignáčová, P. Šittner, V. Novák: IOP Conf. Sci.: Mater. Sci. Eng. 7(1) (2010) 012013-1-8.
- [21] J. Kopeček, S. Sedláková-Ignáčová, K. Jurek, M. Jarošová, J. Drahokoupil, P. Šittner, V. Novák: In: 8th European Symposium on Martensitic Transformations, ESOMAT 2009, Eds: P. Šittner, V. Paidar, L. Heller, H. Seiner, EDP Sciences, Les Ulis Cedex 2009, pp. 02013-1-5.
- [22] J. Kopeček, V. Kopecký, M. Landa, O. Heczko: Mater. Sci. Forum 738-739 (2012) 416-420.
- [23] B. Bártová, D. Schryvers, Z. Q. Yang, S. Ignáčová, P. Šittner: Scripta Mater. 57(1) (2007) 37-40.
- [24] B. Bártová, N. Wiese, D. Schryvers, N. J. Chapman, S. Ignáčová: Acta Mater. 56(16) (2008) 4470-4476.
- [25] Yu.I. Chumlyakov, I.V. Kireeva, E.Yu. Panchenko, E.E. Timofeeva, Z.V. Pobedennaya, S. V. Chusov, I. Karaman, H. Maier, E. Cesari, V.A. Kirillov: Russ. Phys. J. 51(10) (2008) 1016-1036